

Light- and Thermal-Activated Olefin Metathesis of Hindered Substrates

Elisa Ivry,[†] Alexander Frenklah,[†] Yakov Ginzburg,[†] Efrat Levin,[†] Israel Goldberg,[‡] Sebastian Kozuch,[†] N. Gabriel Lemcoff,^{†,§} and Eyal Tzur^{*,||}

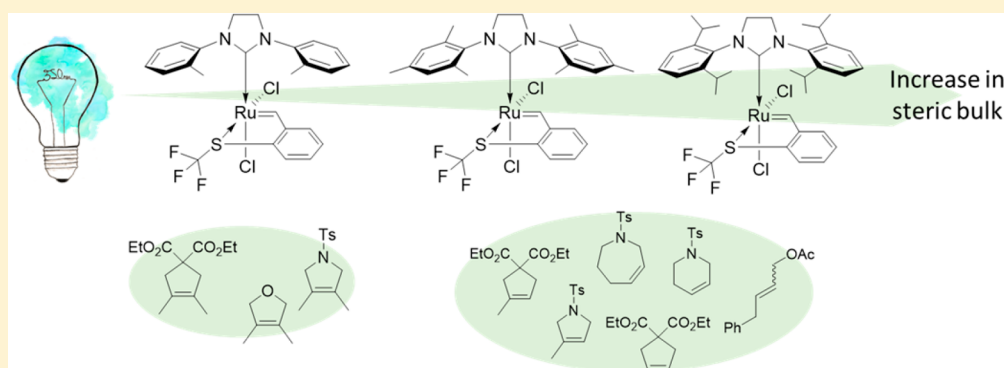
[†]Department of Chemistry, Ben-Gurion University of the Negev, Beer Sheva 84105, Israel

[‡]School of Chemistry, Tel-Aviv University, Tel-Aviv 69978, Israel

[§]Ilse Katz Institute for Nanotechnology, Beer Sheva 8410501, Israel

^{||}Department of Chemical Engineering, Shamoon College of Engineering, Ashdod 77245 Israel

Supporting Information



ABSTRACT: Efficient light- and thermal-activated metathesis reactions of tetra-substituted olefins were obtained by the S-chelated ruthenium precatalyst **Tol-SCF₃**. Its reactivity in a series of benchmark olefin metathesis reactions was compared to previously reported **Mes-SCF₃** and a novel sterically congested S-chelated complex, **Dipp-SCF₃**. **Tol-SCF₃** is thus the first latent catalyst proven to be capable of promoting olefin metathesis of demanding substrates upon light stimulation at room temperature.

INTRODUCTION

Although pioneered decades ago, the world of olefin metathesis is still undergoing continuous development, providing important research and synthetic tools to the field of organic chemistry. One such aspect is the formation of tetra-substituted carbon–carbon double bonds, which was originally found to be challenging when promoted by standard commercially available ruthenium precatalysts, such as **1–3a** (Figure 1). Extensive studies disclosed the great impact of the

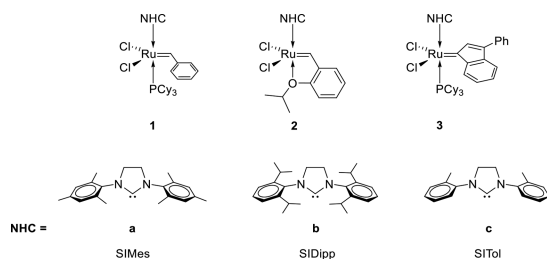


Figure 1. Ruthenium complexes bearing NHC ligands with varying steric hindrance.

steric properties of the *N*-heterocyclic carbene (NHC) ligand on the course of the metathesis reaction.¹ For example, the use of bulky ligand 1,3-bis(2,6-diisopropylphenyl) imidazolidine-2-ylidene (**b**, SIDipp) increased thermal stability and improved activity in metathesis of standard substrates.² In contrast, the reduction of steric bulk around the NHC ligand, by using 1,3-bis(2-methylphenyl)imidazolidine-2-ylidene (**c**, SITol) to produce **1c**, **2c**,³ and **3c**,⁴ allowed increased efficiency in metathesis reactions of sterically demanding olefins.⁵ Other ruthenium scaffolds that may benefit from this strategy are latent ruthenium precatalysts,⁶ such as the sulfur-chelated benzylidenes.⁷ These complexes exhibit a *cis*-dichloro configuration,⁸ which is unreactive toward ring-closing metathesis (RCM), cross-metathesis (CM) and many ring-opening metathesis polymerization (ROMP) reactions at ambient conditions. Activation of these precatalysts has been achieved by means of heat or UV irradiation, which results in the isomerization of the dormant *cis*-dichloro complexes to the active *trans* configuration.^{7a,b} The ability to exploit light as a

Received: September 6, 2017

convenient and powerful energy resource in novel metathesis applications, such as three-dimensional printing of ROMP polymers⁹ or guiding of orthogonal organic reactions,¹⁰ has given quite an impetus to the field of latency. Thus, the expansion of the methodology to include metathesis of sterically demanding substrates is highly desirable.

Herein we report the synthesis of sterically reduced latent precatalyst **Tol-SCF₃**, and its application in light and also thermal activated metathesis of hindered olefins. Sterically encumbered **Dipp-SCF₃** was synthesized as well, and the activities of the two novel complexes were compared to those of previously reported **Mes-SCF₃**¹¹ (Figure 2).

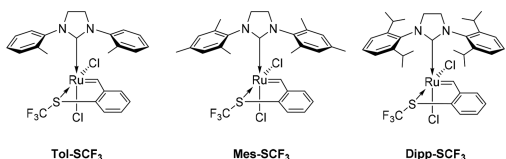
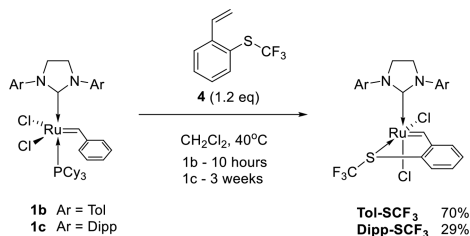


Figure 2. Latent **SCF₃**-chelated precatalysts bearing NHC ligands varying in size investigated in this work.

RESULTS AND DISCUSSION

The new complexes were synthesized by mixing **1b** and **1c** with a slight excess of ligand **4** (Scheme 1) and duly

Scheme 1. Synthesis of Complexes **Tol-SCF₃** and **Dipp-SCF₃**



characterized by NMR, HR-MS, and single crystal X-ray spectroscopy analyses. While the ¹H NMR spectra of **Dipp-SCF₃** and **Mes-SCF₃** exhibited a single benzylidene signal for the *cis*-complex (16.76 and 16.85 ppm, respectively), a careful inspection of the carbene region of **Tol-SCF₃** revealed a main peak at 16.71 ppm accompanied by broad signals at 16.87 ppm. The additional peaks expose the cohabitation of 4 possible rotamers (for full details see the Supporting Information) which can be observed due to hindered rotation around the C_{Ar}-N and Ru-C_{NHC} bonds. A similar behavior was seen in complex **3c**, where the relatively strong interactions of the indenylidene aromatic system with the N-tolyl substituents also prevented free rotation, and heating to 70 °C was required in order to observe the coalescence of the NMR signals.⁴ In contrast, complex **2c** enjoys a high degree of freedom, and all rotamers were averaged at room temperature in the NMR.¹² In line with these observations, a high coalescence temperature was also seen in **Tol-SCF₃**, where the benzylidene and the NHC aromatic rings are stacked upon each other. Heating to 80 °C sharpened the signals to clearly observe two of the rotamers, in a 1:3 ratio (Figure S8 in the Supporting Information). Upon further heating to 130 °C, beginning of coalescence for these two peaks was observed.¹³ Further characterization of the complexes was carried out by crystallographic studies.

Suitable crystals for X-ray diffraction were successfully obtained by slow diffusion of pentane into a dichloromethane solution of the complexes at -20 °C. Both **Dipp-SCF₃** and **Tol-SCF₃** exhibit the predicted *cis*-dichloro configuration with Cl-Ru-Cl angles near 90° (Figure 3). As could be expected,

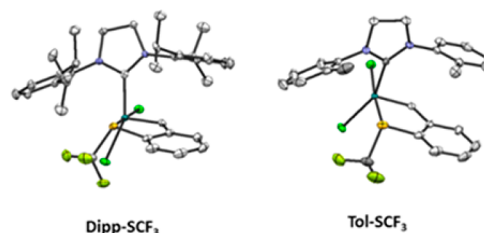


Figure 3. ORTEP diagram of **Tol-SCF₃** and **Dipp-SCF₃**. Ellipsoids are drawn at 50% probability. Hydrogens are omitted for clarity.

the solid-state structure of **Tol-SCF₃** appears as a single conformer, in which the methyl substituents of the tolyl rings are *syn* to one another on the sulfur atom side (complex *syn-a*, Figure S8). Notably, **Tol-SCF₃** is a considerably stable example of a SITol-bearing ruthenium complex. Previously reported complexes bearing NHCs with vacant *ortho* positions on the N-aryl substituent were shown to easily undergo C-H activation, leading to various decomposition products.¹⁴ Such processes are promoted by rotation of the N-substituents to achieve the geometry required for the C-H activation. In previous reports, the rotation of the N-aryl substituent was restricted by placing substituents on the NHC backbone to minimize this decomposition.¹⁵ Interestingly, the rigid structure of **Tol-SCF₃** in its *cis* configuration efficiently prevents rotation of the N-aryl group and thus bestows the complex with additional thermal stability.¹³

A very important aspect of the S-chelated ruthenium complexes is the *cis/trans* isomer interplay. Usually, the *trans* isomer is first obtained as the kinetic product, and heating the solution affords the *cis*-dichloro isomer.¹⁶ While *cis*-dichloro **Tol-SCF₃** was obtained in 10 h, **Dipp-SCF₃** required much harsher conditions, and even after a prolonged heating period of 3 weeks in DCM, some of the kinetic *trans*-isomer could still be observed (Scheme 1). As steric congestion has been shown to influence the *trans-cis* isomerization equilibrium,^{1b,16} it would seem that the high steric hindrance of **Dipp-SCF₃** increases the energy of the transition state between the *trans* and *cis* isomers, thus slowing the isomerization process. To test this hypothesis, the isomerization events were computed using DFT¹⁷ calculations with Gaussian16.¹⁸ Two mechanisms were taken into consideration:⁸ (1) A concerted mechanism, including a pseudorotation of the benzylidene moiety, concomitant with a displacement of the chloride *trans* to the NHC. (2) A dissociative mechanism, where a 14e⁻ intermediate is formed by dissociation of the chelated sulfur, which in turn may re-coordinate in a *cis* configuration after rotation of the benzylidene and relocation of the chloride ligand (Figure S9).

The *syn* rotamers of **Tol-SCF₃**, i.e., *syn-a* (**Tol-SCF₃-α**) and *syn-b* (**Tol-SCF₃-β**), were chosen as the thermodynamic products due to the observed **Tol-SCF₃** configuration in the solid state (*vide supra*) and as they were also shown to be the dominant species in solution of **2c**.¹² According to Table 1, it would appear that in DCM **Tol-SCF₃-α** is predicted to show no distinct preference for any of the mechanisms; however,

Table 1. ΔE [kcal/mol] for the SCF_3 -Chelated Species in the Two *cis*–*trans* Isomerization Mechanisms^a

pathway	complex	DCM			<i>cis</i>	toluene			
		TS1	int.	TS2		TS1	int.	TS2	<i>cis</i>
concerted	Tol- SCF_3 - α	29.3			-5.8	29.5			-3.8
	Tol- SCF_3 - β	26.3			-4.3	26.8			-2.2
	Mes- SCF_3	26.3			-8.3	26.4			-6.4
	Dipp- SCF_3	29.2			-4.3	31.0			-2.8
dissociative	Tol- SCF_3 - α	19.2	14.7	29.0	-5.8	20.1	15.1	30.5	-3.8
	Tol- SCF_3 - β	20.6	15.7	34.4	-4.3	21.3	16.0	36.5	-2.2
	Mes- SCF_3	18.9	13.1	32.5	-8.3	21.0	12.9	34.0	-6.4
	Dipp- SCF_3	18.7	12.3	31.3	-4.3	19.3	12.5	32.5	-2.8

^aCalculated for DCM and toluene, solvation model PCM with reference to the *trans* isomer.

Tol- SCF_3 - β showed a much lower energy for the transition state in the concerted mechanism. The energy required for the rotation of the NHC from *trans*-Tol- SCF_3 - α to *trans*-Tol- SCF_3 - β is ~ 14.50 kcal/mol. Therefore, it may be assumed that the two rotamers can indeed interconvert in order to produce the lower energy transition state required for the isomerization process. Tol- SCF_3 , Mes- SCF_3 , and Dipp- SCF_3 show a preference toward the concerted mechanism, in which, the ΔE for the isomerization of Dipp- SCF_3 is higher by ~ 3 kcal/mol. This may account for the very slow isomerization of the *trans*-Dipp- SCF_3 to the *cis*-Dipp- SCF_3 isomer.

Following their full structural characterization, the activities of the precatalysts were compared in a series of benchmark RCM reactions, including sterically hindered substrates. The reactions were all run in toluene-*d*₈ at 0.1 M substrate concentration. At room temperature, no RCM activity was observed for any of the catalysts and substrates checked, confirming the expected latency of the precatalysts. Thermal activation was effected by heating the reaction mixtures to 80 °C. The kinetic profiles of the reactions were monitored by ¹H NMR (500 MHz) and are presented in Figures 4–6. In

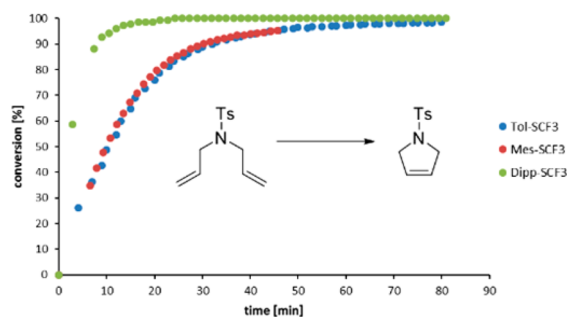


Figure 4. Kinetic profile of RCM of *N,N*-diallyltosyl amine. Toluene-*d*₈, 0.1M, 80 °C, 2 mol % cat.

accordance with literature precedents, RCM reactions that afford doubly (Figure 4) and triply (Figure 5) substituted olefins were faster when catalyzed by Dipp- SCF_3 . Moreover, the results obtained using Dipp- SCF_3 make this new complex the most efficient olefin metathesis catalyst in the family of S-chelated benzylidenes for this type of reactions. However, when diethyl bis(2-methylallyl)malonate was used as the substrate, the trend was reversed, and Tol- SCF_3 was the best performer (Figure 6). Tol- SCF_3 not only was the fastest to initiate but also gave a substantially higher conversion compared to the other complexes within the reaction time

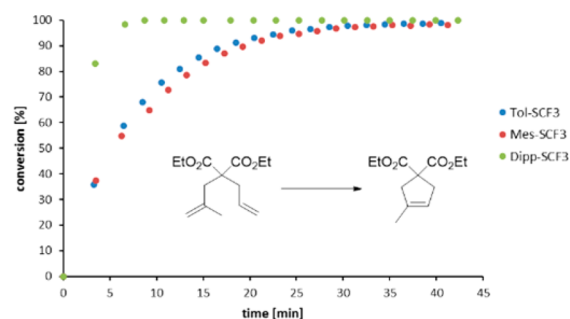


Figure 5. Kinetic profile of RCM of diethyl 2-allyl-2-(2-methylallyl)malonate. Toluene-*d*₈, 0.1M, 80 °C, 2 mol % cat.

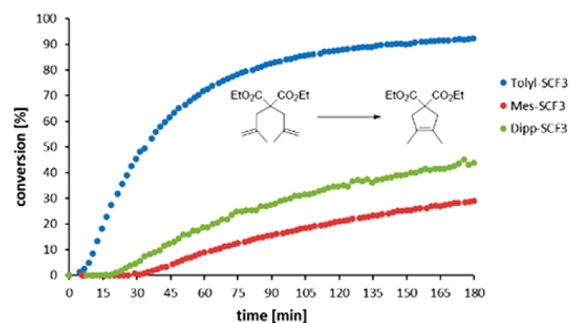


Figure 6. Kinetic profile of RCM of diethyl 2,2-bis(2-methylallyl)malonate. Toluene-*d*₈, 0.1M, 80 °C, 2 mol % cat.

frame of 3 h. Interestingly, except for Tol- SCF_3 , a significant induction period was observed. As this induction period is only evident with the most hindered substrate, we propose that this unexpected behavior is a result of steric hindrance within the catalytic sphere.^{12,19} For the S-chelated precatalysts, two steps are required to generate an active complex. First, the complex must isomerize to an active species, i.e., the *trans* precatalyst or directly the *trans* 14e⁻ intermediate. Second, the olefin substrate needs to coordinate (either in an associative or dissociative manner)²⁰ to the ruthenium center to produce a species which will eventually lead to a productive RCM pathway. It is reasonable to assume that the higher the steric congestion, the slower the second coordination step. Therefore, we suggest that in the case of hindered olefins the second step has the highest transition state, causing initiation to be significantly affected by steric volume. This may also explain the reduced induction period observed for Tol- SCF_3 , which can best accommodate the incoming olefin. In contrast, Dipp- SCF_3 initiates and performs more efficiently than Mes- SCF_3 .

Table 1 suggests that a slightly lower energy is required to obtain the $14e^-$ intermediate of **Dipp-SCF₃** in toluene, allowing for more productive metathesis encounters with the substrate and diminishing the induction period. This is an example of the delicate interplay between both processes (precatalyst activation and substrate coordination) required to promote latent olefin metathesis of hindered substrates.

The scope of the reaction was further explored with several RCM and CM substrates, supporting the previously observed trend (Table 2). **Dipp-SCF₃** was the fastest catalyst of the

Table 2. RCM and CM Reactions Promoted by SCF₃-Chelated Complexes by Thermal Activation^a

entry	substrate	product	complex	conv. (%)
1			Tol-SCF₃	70
			Mes-SCF₃	23
			Dipp-SCF₃	98
2			Tol-SCF₃	90
			Mes-SCF₃	34
			Dipp-SCF₃	100
3			Tol-SCF₃	52
			Mes-SCF₃	71
			Dipp-SCF₃	100
4			Tol-SCF₃	91
			Mes-SCF₃	90
			Dipp-SCF₃	100
5 ^b			Tol-SCF₃	59
			Mes-SCF₃	42
			Dipp-SCF₃	51
6 ^b			Tol-SCF₃	94 (83) ^c
			Mes-SCF₃	20
			Dipp-SCF₃	38
7 ^d			Tol-SCF₃	56
			Mes-SCF₃	55
			Dipp-SCF₃	85
8 ^e			Tol-SCF₃	56 ^f
			Mes-SCF₃	48
			Dipp-SCF₃	34

^aReaction conditions: 0.1 M substrate in toluene, 1 mol % cat., 15 min at 80 °C. Conversions determined by GC-MS. ^bReaction conditions: 5 mol % cat., 120 min. ^cReaction conditions: 0.4 mol % cat. ^dMesitylene as internal standard and 2 equiv of cis-1,4-diacetoxy-2-butene. ^eReaction conditions: 5 mol % cat., 120 min, mesitylene as internal standard and 3 equiv of allylbenzene. ^fMeasured by ¹H NMR.

group yielding almost complete conversions within 15 min under the thermal activating conditions for di- and trisubstituted olefins (entries 1–4). Once again, when demanding tetra-substituted substrates were used, **Tol-SCF₃** excelled (entries 5–6). The limits of the RCM reaction of *N,N*-bis-2-methylallyl tosyl amine using **Tol-SCF₃** (entry 6) were also tested at lower catalyst loadings. Thus, 0.4 mol % **Tol-SCF₃** promoted 83% conversion within 60 min at 100 °C. In addition, a CM reaction produced satisfactory results as well, with **Dipp-SCF₃** affording 85% conversion within 15 min

(entry 7). When a hindered olefin was used as a CM partner (entry 8), **Tol-SCF₃** and **Mes-SCF₃** maintained their efficiency, while that of **Dipp-SCF₃** dropped dramatically. The results highlight the usefulness of **Tol-SCF₃** in challenging reactions where latency may be required.

Finally, the appealing light activation of the precatalysts by UV irradiation at 350 nm was examined (Table 3). To our

Table 3. RCM Reactions Promoted by SCF₃-Chelated Complexes under 350 nm UV Irradiation^{a,21}

entry	product	time	cat. (mol%)	complex	conv. (%)
1		30 min	0.5	Tol-SCF₃	58
				Mes-SCF₃	90
				Dipp-SCF₃	94
2		35 min	2	Tol-SCF₃	81
				Mes-SCF₃	100
				Dipp-SCF₃	94
3		6 h	5	Tol-SCF₃	91
				Mes-SCF₃	0
				Dipp-SCF₃	0
4 ^b		10 h	5	Tol-SCF₃	92
				Mes-SCF₃	7
				Dipp-SCF₃	9

^aReactions were conducted in DCM-*d*₂, 0.1M; conversions determined by ¹H NMR (500 MHz). ^bToluene-*d*₈.

satisfaction, the behavior for light-promoted RCM of olefins fell in line with the results obtained for the thermal activation and provided good results with precatalysts **Mes-SCF₃** and **Dipp-SCF₃** with unhindered olefins. **Tol-SCF₃** also maintained its high effectiveness in the RCM of tetra-substituted olefins, but **Mes-SCF₃** and **Dipp-SCF₃** substantially underperformed compared to thermal activation (entries 5–6 in Table 2 and entries 3 and 4 in Table 3). Although RCM under UV irradiation required longer reaction periods, especially for tetra-substituted olefins, our results show that **Tol-SCF₃** is the only catalyst that can perform efficient light-promoted RCM reactions in sterically challenging substrates.

CONCLUSIONS

S-chelated complexes bearing NHC ligands varying in size have been synthesized and fully characterized. Solid and solution state analyses revealed the influence of the bulkiness of the NHC ligand on the complexes' structures and their inherent stability. These characteristics directly affect key process of the metathesis catalysis. The complex bearing the smallest NHC, **Tol-SCF₃**, provided excellent results in thermal- and light-induced metathesis of hindered olefins. As such, **Tol-SCF₃** is the first light-activated latent olefin metathesis catalyst that can efficiently perform metathesis in sterically demanding substrates. The complex bearing the bulkiest NHC, **Dipp-SCF₃**, provided the best results for di- and trisubstituted benchmark RCM reactions. These novel complexes expand the scope and efficiency of the sulfur-chelated precatalyst family for latent olefin metathesis catalysis applications.

■ EXPERIMENTAL SECTION

General. All reagents were of reagent-grade quality, purchased commercially from Sigma-Aldrich, Sterm, or Alfa Aesar, and used without further purification. All solvents were dried and distilled prior to use. Purifications by column chromatography were performed on Davisil Chromatographic silica media (40–6 μm). TLC analyses were performed using Merck precoated silica gel (0.2 mm) aluminum [backed] sheets. Gas chromatography data was obtained using an Agilent 6850 GC equipped with an Agilent 5973 MSD working under standard conditions and an Agilent HP5-MS column. NMR spectra were recorded on Bruker DPX400 or DPX500 instruments; chemical shifts, given in ppm, are relative to the residual solvent peak. HRMS data were obtained using a Bruker Daltonics Ion Trap MS Esquire 3000 Plus equipped with APCI (Atmospheric Pressure Chemical Ionization). Irradiation experiments were carried out using a Rayonet RPR-200 instrument with 350.0 nm lamp and were carried out in NMR tube.

(Trifluoromethyl)(2-vinylphenyl)sulfane (4). New synthesis procedure for 4:¹¹ In a dry flask, methyl triphenylphosphonium iodide (11.79 g, 29.02 mmol) was stirred in dry ether (100 mL), at 0 °C, under N₂ atmosphere. KO^tBu (3.86 g, 34.40 mmol) was added in one portion. The solution was stirred at 0 °C for 15 min. 2-((Trifluoromethyl)thio)benzaldehyde (5.00 g, 24.25 mmol) was added in one portion. The solution was stirred for 3 h, until the reaction was judged complete by GC-MS. Saturated NaHCO₃ solution (100 mL) was added, and the phases were separated. The aqueous phase was extracted with ether (3 \times 50 mL). The combined organic layers were washed with water and brine and dried over MgSO₄. The drying reagent was filtered off, and the liquid was stored at –18 °C overnight. The precipitated triphenylphosphine oxide was filtered off, and the solvent was evaporated. The crude product was purified on silica gel column with petroleum ether as eluent. 4 was obtained as a colorless oil (2.64 g, 53%). The NMR and GC-MS spectra were in agreement with previous results.¹¹

Ru(SIMes)(=CHPhSCF₃)Cl₂ (Mes-SCF₃). Prepared according to previously reported literature procedure.¹¹

Ru(SITol)(=CHPhSCF₃)Cl₂ (Tol-SCF₃). In the glovebox, Tol-Grubbs (1c) (300 mg, 0.38 mmol) was dissolved in dry DCM (20 mL) followed by addition of ligand 4 (109 mg, 0.53 mmol). The pressure tube was sealed, and the reaction mixture was refluxed overnight. The solvent was removed under vacuum, and the crude was redissolved in minimal amount of DCM. Ether was slowly added until precipitation of a purple-blue solid was obtained. After the suspension was sonicated a few minutes, the solvent was decanted. Benzene was added, and the solution was sonicated for 2 h. The solid was filtered and washed several times with benzene, followed by drying under high vacuum for 5 days. Tol-SCF₃ was obtained as a light blue solid (162 mg, 70%). Crystals suitable for X-ray analysis were obtained by slow diffusion of pentane into a DCM solution of the product in –20 °C. ¹H NMR (400 MHz, CD₂Cl₂): δ 16.88–16.72 (m, 1H), 8.46 (s, 0.5H), 7.76–7.62 (m, 3H), 7.51–7.47 (m, 3.5H), 7.40–7.36 (m, 1H), 7.33–7.25 (m, 3H) 6.80 (d, J = 7.6 Hz, 1H), 6.72 (d, J = 7.2, 1H), 4.27 (bs, 1H), 4.16–4.07 (m, 1H), 4.05–3.98 (m, 1H), 3.94–3.86 (m, 1H), 2.58 (s, 3H), 1.26 (bs, 3H). ¹³C NMR (101 MHz, CD₂Cl₂) δ 290.6, 208.8, 155.4, 138.9, 136.0, 133.2, 132.9, 131.4, 131.3, 131.1, 130.6, 129.8, 129.4, 128.8, 128.5, 127.7, 127.3, 127.2, 126.0, 125.6, 125.2, 122.7, 52.5, 52.0, 19.0, 16.4. ¹⁹F NMR (376 MHz, CD₂Cl₂): δ –41.1. HRMS m/z calcd for [C₂₅H₂₃ClF₃N₂RuS]⁺ (M – Cl)⁺: 577.0261, found: 577.0204. The fractions observed in the integrals of the ¹H NMR spectrum are due to the presence of minor and major rotamers.

Ru(SIDipp)(=CHPhSCF₃)Cl₂ (Dipp-SCF₃). In the glovebox, Dipp-Grubbs (1b) (500 mg, 0.54 mmol) was dissolved in dry DCM (20 mL) followed by addition of ligand 4 (190 mg, 0.93 mmol). The reaction mixture was refluxed for 3 weeks. The solvent was removed under vacuum. *cis*-Dipp-SCF₃ was purified by flash chromatography using 7:1 to 7:2 hexane/acetone as eluent to give gray-green solid (171.0 mg, 29%). Crystals suitable for X-ray analysis were obtained by slow diffusion of pentane into a DCM solution of

the product in –20 °C. ¹H NMR (400 MHz, CD₂Cl₂): δ 16.76 (s, 1H), 7.66 (d, J = 7.8 Hz, 1H), 7.56 (dd, J = 15.3, 7.6 Hz, 2H), 7.46 (dd, J = 7.8, 1.3 Hz, 1H), 7.37–7.33 (m, 2H), 7.28 (t, J = 7.5 Hz, 1H), 7.22 (t, J = 7.7 Hz, 1H), 6.86 (d, J = 7.6 Hz, 1H), 6.48 (dd, J = 7.7, 1.1 Hz, 1H), 4.33–4.03 (m, 5H), 3.91 (m, 1H), 3.33 (m, 1H), 2.29 (m, 1H), 1.65 (d, J = 6.5, 3H), 1.58 (m, 6H), 1.24 (d, J = 6.7, 6H), 1.24 (d, J = 6.8, 6H) 1.19 (d, J = 6.9, 3H) 0.97, (d, J = 6.7, 3H), 0.41 (d, J = 6.7, 3H). ¹³C NMR (100 MHz, CD₂Cl₂): δ 286.1, 213.8, 154.9, 151.2, 149.8, 147.7, 145.9, 136.4, 132.4, 132.2, 131.7, 131.3, 131.0, 130.7, 130.1, 127.0, 126.3, 125.6, 125.4, 124.9, 123.8, 54.6, 29.7, 29.6, 29.2, 28.8, 28.4, 28.1, 27.2, 26.6, 24.6, 23.2, 22.4, 21.6. ¹⁹F NMR (377 MHz, CD₂Cl₂): δ –75.77. HRMS m/z calcd for [C₃₅H₄₃Cl₂F₃N₂RuSNa]⁺: 775.14118, found 775.13983.

General Procedure for RCM Reaction. All substrates which were not commercially available were synthesized according to known procedures from the literature. In the glovebox, a solution of the substrate in the appropriate solvent (0.1M) was added to ruthenium complex (0.5, 1, 2, or 5 mol %). The mixture was then transferred to an NMR tube or a vial, which in turn was placed in an 80 °C heating bath or in a Rayonet photoreactor. Conversion was monitored by GC-MS or ¹H NMR.

General Procedure for CM Reaction. All substrates which were not commercially available were synthesized according to known procedures from the literature. In the glovebox, a solution of the substrates in the appropriate solvent (0.1M) was added to ruthenium complex (1 or 5 mol %). The mixture was placed in an 80 °C heating bath. Conversion was monitored by GC-MS using mesitylene (1.5 equiv) as internal standard.

Computational Details. The DFT geometry optimization was performed using B97D3/Def2-SVP. Final geometries were confirmed to be minimum energy structures through frequency calculations. Reaction pathway was also confirmed using IRC calculations. Single point calculations were performed using MN15/Def2-TZVP. Solvent effects have been estimated in single point calculations based on PCM model for DCM and toluene.

■ ASSOCIATED CONTENT

Supporting Information

The Supporting Information is available free of charge on the ACS Publications website at DOI: 10.1021/acs.organomet.7b00677.

NMR spectra, MS data and X-ray data of two complexes, computational energy plot, and ΔG values of Table 1 (PDF)

Atomic coordinate files (XLSX, XYZ)

Accession Codes

CCDC 1564124–1564125 contain the supplementary crystallographic data for this paper. These data can be obtained free of charge via www.ccdc.cam.ac.uk/data_request/cif, or by emailing data_request@ccdc.cam.ac.uk, or by contacting The Cambridge Crystallographic Data Centre, 12 Union Road, Cambridge CB2 1EZ, UK; fax: +44 1223 336033.

■ AUTHOR INFORMATION

Corresponding Author

*E-mail: eyalt@sce.ac.il.

ORCID

Israel Goldberg: 0000-0002-3117-0534

Sebastian Kozuch: 0000-0003-3070-8141

N. Gabriel Lemcoff: 0000-0003-1254-1149

Notes

The authors declare no competing financial interest.

ACKNOWLEDGMENTS

E.T. acknowledges grant No. 14/Y16/T1/D3/Yr2 provided by the Shamoon College of Engineering, Ashdod, Israel. The Israel Science Foundation is gratefully acknowledged for partial funding of this work (Grant No. 537/14).

REFERENCES

- (1) (a) Credendino, R.; Poater, A.; Ragone, F.; Cavallo, L. *Catal. Sci. Technol.* **2011**, *1*, 1287–1297. (b) Pump, E.; Leitgeb, A.; Kozłowska, A.; Torvisco, A.; Falivene, L.; Cavallo, L.; Grela, K.; Slugovc, C. *Organometallics* **2015**, *34*, 5383–5392. (c) Gómez-Suárez, A.; Nelson, D. J.; Nolan, S. P. *Chem. Commun.* **2017**, *53*, 2650–2660.
- (2) (a) Fürstner, A.; Ackermann, L.; Gabor, B.; Goddard, R.; Lehmann, C. W.; Mynott, R.; Stelzer, F.; Thiel, O. R. *Chem. - Eur. J.* **2001**, *7*, 3236–3253. (b) Courchay, F. C.; Sworen, J. C.; Wagener, K. B. *Macromolecules* **2003**, *36*, 8231–8239. (c) Clavier, H.; Urbina-Blanco, C. A.; Nolan, S. P. *Organometallics* **2009**, *28*, 2848–2854.
- (3) (a) Stewart, I. C.; Ung, T.; Pletnev, A. A.; Berlin, J. M.; Grubbs, R. H.; Schrodi, Y. *Org. Lett.* **2007**, *9*, 1589–1592. (b) Stewart, I. C.; Douglas, C. J.; Grubbs, R. H. *Org. Lett.* **2008**, *10*, 441–444.
- (4) Torborg, C.; Szczepaniak, G.; Zieliński, A.; Malińska, M.; Woźniak, K.; Grela, K. *Chem. Commun.* **2013**, *49*, 3188–3190.
- (5) For other examples of efficient ruthenium catalysts in RCM of sterically demanding substrates, see (a) Berlin, J. M.; Campbell, K.; Ritter, T.; Funk, T. W.; Chlenov, A.; Grubbs, R. H. *Org. Lett.* **2007**, *9*, 1339–1342. (b) Stenne, B.; Timperio, J.; Savoie, J.; Dudding, T.; Collins, S. K. *Org. Lett.* **2010**, *12*, 2032–2035. (c) Peeck, L. H.; Plenio, H. *Organometallics* **2010**, *29*, 2761–2766. (d) Bantreil, X.; Schmid, T. E.; Randall, R. A. M.; Slawin, A. M. Z.; Cazin, C. S. J. *Chem. Commun.* **2010**, *46*, 7115–7117. (e) Songis, O.; Slawin, A. M. Z.; Cazin, C. S. J. *Chem. Commun.* **2012**, *48*, 1266–1268.
- (6) (a) Szadkowska, A.; Grela, K. *Curr. Org. Chem.* **2008**, *12*, 1631–1647. (b) Monsaert, S.; Lozano Vila, A.; Drozdak, R.; Van Der Voort, P.; Verpoort, F. *Chem. Soc. Rev.* **2009**, *38*, 3360–3372.
- (7) For latent complexes containing benzylidene thio-ethers, see (a) Ben-Asuly, A.; Tzur, E.; Diesendruck, C. E.; Sigalov, M.; Goldberg, I.; Lemcoff, N. G. *Organometallics* **2008**, *27*, 811–813. (b) Ben-Asuly, A.; Aharoni, A.; Diesendruck, C. E.; Vidavsky, Y.; Goldberg, I.; Straub, B. F.; Lemcoff, N. G. *Organometallics* **2009**, *28*, 4652–4655. (c) Diesendruck, C. E.; Iliashevsky, O.; Ben-Asuly, A.; Goldberg, I.; Lemcoff, N. G. *Macromol. Symp.* **2010**, *293*, 33–38. (d) Grudzień, K.; Żukowska, K.; Malińska, M.; Woźniak, K.; Barbasiewicz, M. *Chem. - Eur. J.* **2014**, *20*, 2819–2828. (e) Mikus, M. S.; Torker, S.; Xu, C.; Li, B.; Hoveyda, A. H. *Organometallics* **2016**, *35*, 3878–3892. For other olefin metathesis complexes bearing thioethers or thiolate ligands (latent and nonlatent), see (f) Occhipinti, G.; Hansen, F. R.; Törnroos, K. W.; Jensen, V. R. *J. Am. Chem. Soc.* **2013**, *135*, 3331–3334. (g) Khan, R. K. M.; Torker, S.; Hoveyda, A. H. *J. Am. Chem. Soc.* **2013**, *135*, 10258–10261. (h) McKinty, A. M.; Lund, C.; Stephan, D. W. *Organometallics* **2013**, *32*, 4730–4732. (i) McKinty, A. M.; Stephan, D. W. *Dalton Trans.* **2016**, *45*, 3844–3852.
- (8) The following paper summarizes many complexes with *cis*-dichloro configuration: Pump, E.; Cavallo, L.; Slugovc, C. *Monatsh. Chem.* **2015**, *146*, 1131–1141.
- (9) (a) Tzur, E.; Lemcoff, N. G. Latent ruthenium olefin metathesis catalysts for ROMP. In *Handbook of Metathesis*; Grubbs, R. H., Wenzel, A. G., O'Leary, D. J., Khosravi, E., Eds.; WILEY-VCH: Weinheim, Germany, 2015; Vol. 3, pp 283–312. (b) Teator, A. J.; Lastovickova, D. N.; Bielawski, C. W. *Chem. Rev.* **2016**, *116*, 1969–1992. (c) Saha, S.; Ginzburg, Y.; Rozenberg, I.; Iliashevsky, O.; Ben-Asuly, A.; Lemcoff, N. G. *Polym. Chem.* **2016**, *7*, 3071–3075. (d) Reisch, M. *Chem. Eng. News* **2016**, *94* (43), 34. <https://cen.acs.org/articles/94/i43/PolySpectra.html>
- (10) (a) Vidavsky, Y.; Lemcoff, N. G. *Beilstein J. Org. Chem.* **2010**, *6*, 1106–1119. (b) Levin, E.; Mavila, S.; Eivgi, O.; Tzur, E.; Lemcoff, N. G. *Angew. Chem., Int. Ed.* **2015**, *54*, 12384–12388. (c) Sutar, R. L.; Levin, E.; Butilkov, D.; Goldberg, I.; Reany, O.; Lemcoff, N. G. *Angew. Chem., Int. Ed.* **2016**, *55*, 764–767.
- (11) Ginzburg, Y.; Anaby, A.; Vidavsky, Y.; Diesendruck, C. E.; Ben-Asuly, A.; Goldberg, I.; Lemcoff, N. G. *Organometallics* **2011**, *30*, 3430–3437.
- (12) Stewart, I. C.; Benitez, D.; O'Leary, D. J.; Tkatchouk, E.; Day, M. W.; Goddard, W. A., III; Grubbs, R. H. *J. Am. Chem. Soc.* **2009**, *131*, 1931–1938.
- (13) The boiling point of the solvent (TCE-*d*₂, 146.5 °C) prevented heating inside the NMR instrument above 130 °C, even though the complex was quite stable even at these high temperatures and did not show signs of decomposition. However, complete coalescence could not be achieved at the limiting temperature.
- (14) (a) Vehlou, K.; Gessler, S.; Blechert, S. *Angew. Chem., Int. Ed.* **2007**, *46*, 8082–8085. (b) Herbert, M. B.; Lan, Y.; Keitz, B. K.; Liu, P.; Endo, K.; Day, M. W.; Houk, K. N.; Grubbs, R. H. *J. Am. Chem. Soc.* **2012**, *134*, 7861–7866.
- (15) (a) Kuhn, K. M.; Bourg, J.-B.; Chung, C. K.; Virgil, S. C.; Grubbs, R. H. *J. Am. Chem. Soc.* **2009**, *131*, 5313–5320. (b) Grisi, F.; Mariconda, A.; Costabile, C.; Bertolasi, V.; Longo, P. *Organometallics* **2009**, *28*, 4988–4995. (c) Peretto, A.; Costabile, C.; Longo, P.; Grisi, F. *Organometallics* **2014**, *33*, 2747–2759. Grela and co-workers showed that complex **3c** presented increased thermal stability due to use of the indenylidene moiety, see ref 4.
- (16) Aharoni, A.; Vidavsky, Y.; Diesendruck, C. E.; Ben-Asuly, A.; Goldberg, I.; Lemcoff, N. G. *Organometallics* **2011**, *30*, 1607–1615.
- (17) (a) Yu, H. S.; He, X.; Li, S. L.; Truhlar, D. G. *Chem. Sci.* **2016**, *7*, 5032–5051. (b) Grimme, S. *J. Comput. Chem.* **2006**, *27*, 1787–1799.
- (18) Frisch, M. J.; Trucks, G. W.; Schlegel, H. B.; Scuseria, G. E.; Robb, M. A.; Cheeseman, J. R.; Scalmani, G.; Barone, V.; Petersson, G. A.; Nakatsuji, H.; Li, X.; Caricato, M.; Marenich, A. V.; Bloino, J.; Janesko, B. G.; Gomperts, R.; Mennucci, B.; Hratchian, H. P.; Ortiz, J. V.; Izmaylov, A. F.; Sonnenberg, J. L.; Williams-Young, D.; Ding, F.; Lipparini, F.; Egidi, F.; Goings, J.; Peng, B.; Petrone, A.; Henderson, T.; Ranasinghe, D.; Zakrzewski, V. G.; Gao, J.; Rega, N.; Zheng, G.; Liang, W.; Hada, M.; Ehara, M.; Toyota, K.; Fukuda, R.; Hasegawa, J.; Ishida, M.; Nakajima, T.; Honda, Y.; Kitao, O.; Nakai, H.; Vreven, T.; Throssell, K.; Montgomery, J. A., Jr.; Peralta, J. E.; Ogliaro, F.; Bearpark, M.; Heyd, J. J.; Brothers, E. N.; Kudin, K. N.; Staroverov, V. N.; Kobayashi, R.; Normand, J.; Raghavachari, K.; Rendell, A.; Burant, J. C.; Iyengar, S. S.; Tomasi, J.; Cossi, M.; Millam, J. M.; Klene, M.; Adamo, C.; Cammi, R.; Ochterski, J. W.; Martin, R. L.; Morokuma, K.; Farkas, O.; Foresman, J. B.; Fox, D. J. *Gaussian 16*, revision A.03; Gaussian, Inc.: Wallingford CT, 2016.
- (19) Costabile, C.; Cavallo, L. *J. Am. Chem. Soc.* **2004**, *126*, 9592–9600.
- (20) Thiel, V.; Hendann, M.; Wannowius, K.-J.; Plenio, H. *J. Am. Chem. Soc.* **2012**, *134*, 1104–1114.
- (21) As control experiments to exclude the thermal activation, identical samples were covered with aluminum foil and were placed next to the reaction tubes inside the Rayonet photoreactor. As expected, no RCM was observed for these samples.